



# Baltic Sea Surface Temperature Analysis 2022: A Study of Marine Heatwaves and Overall High Seasonal Temperatures

Anja Lindenthal<sup>1</sup> and Claudia Hinrichs<sup>1</sup>, Simon Jandt-Scheelke<sup>1</sup>, Tim Kruschke<sup>1</sup>, Priidik Lagemaa<sup>3</sup>, Eefke M. van der Lee<sup>2</sup>, Helen E. Morrison<sup>2</sup>, Tabea R. Panteleit<sup>1</sup>, Urmars Raudsepp<sup>3</sup>

5 <sup>1</sup>Federal Maritime and Hydrographic Agency, Hamburg, 20539, Germany

<sup>2</sup>Federal Maritime and Hydrographic Agency, Rostock, 18057, Germany

<sup>3</sup>Department of Marine Systems, Tallinn University of Technology, Tallinn, 12618, Estonia

*Correspondence to:* Claudia Hinrichs ([claudia.hinrichs@bsh.de](mailto:claudia.hinrichs@bsh.de)); Helen E. Morrison ([helen.morrison@bsh.de](mailto:helen.morrison@bsh.de))

**Abstract.** In 2022, large parts of the Baltic Sea surface experienced the third-warmest to the warmest summer and autumn  
10 temperatures since 1997. Warm temperature anomalies are a precondition for marine heatwaves (MHWs), which are discrete  
periods of anomalous high temperatures relative to the usual local conditions. Here, we describe the overall sea surface  
temperature (SST) conditions observed in the Baltic Sea in 2022 and provide a spatio-temporal description of surface MHW  
events based on remote sensing, model reanalyses and in-situ station data. Most MHWs, four and locally even up to seven  
15 values up to 4.6 °C above the climatological mean. The Northern Baltic Proper and the Gulf of Bothnia were impacted by  
mainly two MHWs at maximum intensities of 7.3 °C and 9.6 °C, respectively. Our results also reveal that MHWs in the  
upper layer occur at a different period than at the bottom layers and are likely driven by different mechanisms. Results from  
the case studies at two exemplary stations ‘Lighthouse Kiel (LT Kiel)’ and ‘Northern Baltic’ show a significant increase of  
MHW occurrences of +0.7 MHW events per decade at LT Kiel from 1989 to 2022 and of +0.64 MHW events per decade  
20 from 1993 to 2022 at Northern Baltic. Moreover, the expected future increase of MHW occurrences is discussed based on a  
statistical analysis at both locations.

## 1 Introduction

Global warming has manifested itself through the increase of ocean heat content (OHC) by about 350 ZJ in the upper 2000  
meters from 1958 to 2019 with the year 2022 being the warmest on record (Cheng et al., 2022; WMO, 2023).  
25 Simultaneously, marine heatwaves (MHWs), the extreme events of high water temperature (Hobday et al., 2016), have  
increased in their frequency, duration, spatial extent and intensity during the past four decades (Sun et al., 2023). In 2022,  
MHWs were recorded on 58 % of the ocean surface (WMO, 2023).

The global mean air temperature in 2022 was 1.15 [1.02–1.28] °C above the 1850–1900 average, resulting in the year 2022  
to be the fifth or sixth warmest year in the 173-year instrumental record (WMO, 2023). We could hence expect the marginal  
30 seas like the Baltic Sea to experience high sea surface temperatures (SST) as well. This hypothesis is supported by the study



which showed that the extremely warm weather conditions in winter 2019/20 resulted in an unusually high heat content anomaly in the upper 50 m layer of the Baltic Sea (Raudsepp et al., 2022). Thus, a large-scale weather pattern could have a detectable response to the physical conditions of the Baltic Sea.

Belkin (2009) showed that the Baltic Sea is one of the seas which have warmed fastest in the last decades with a warming of 1.35 K between 1982 and 2006, i.e., 0.54 °C per decade. In our BSH data (product ref. no. 1 in Table 1) we see a trend of 0.58 °C per decade for the period 1990–2022 (based on annual means derived from satellite data, not shown). Local air sea heat exchange is the main physical factor that determines the surface layer water temperature and heat content in the Baltic Sea (Raudsepp et al., 2022). A permanent halocline at the depth of 60–80 m (Väli et al., 2013) limits heat exchange between surface and lower layers. Further on, limited water exchange of the Baltic Sea with the open ocean through the Skagerrak potentially reduces heat transport between the sea and the ocean.

MHWs are usually detected using remotely sensed SST. High SST could affect phytoplankton production, while unprecedented high temperatures in the subsurface layers of the sea could have even more devastating effects on the marine ecosystem (Kauppi et al., 2023). Subsurface layer MHWs can be detected using temperature moorings, though unfortunately these moorings provide only point measurements. Numerical models enhance the possibility for studying dynamics of MHWs including their extension to the subsurface layers of the ocean. In this study we utilize remote sensing, model reanalyses and in-situ station data for the spatio-temporal description of the MHWs in the Baltic Sea in 2022. So far, there are generally only a few studies about MHWs in the Baltic Sea (Goebeler et al., 2022; She et al., 2020). In addition to the detailed description of MHWs in 2022 we extended our study by providing climatology of the MHWs based on mooring station data.

## 2 Data and Methods

### 2.1 Satellite data

Maps of SST satellite data, as, for example, used by The BACC Author Team (2008) and Gröger et al. (2022), are compiled daily by the satellite data service at BSH (product ref. no. 1 in Table 1). These data are recorded as radiances by the third generation of the Advanced Very High Resolution Radiometer (AVHRR/3) in channels 4 and 5 centered at wavelengths 10.8 µm and 12.0 µm in the thermal infrared respectively (EUMETSAT, 2015). The AVHRR/3 instruments used are flown aboard the polar orbiting NOAA-19 and MetOp B satellites providing a spatial resolution of 1.1 km directly below the instrument (in nadir), swath widths of 1,447 km and orbital periods of 100 minutes (EUMETSAT, 2015; Minnett et al., 2019). This results in generally 8 or 9 daytime passes over the Baltic and North Sea area per day. The raw data (level 0) are received directly from EUMETSAT 90 minutes after flyover and processed using automated, standardized correction procedures (atmospheric correction, cloud masking, georeferencing etc.). Additionally, each flyover is corrected manually in order to preserve as much data as possible whilst eliminating any faulty or cloudy pixels. All available single images from a calendar day are combined and averaged, on a single pixel basis, into one daily-mean image. These daily images are then



used to produce a weekly analysis on an operational basis. This weekly analysis is produced on an equidistant grid of 58 by 74 cells in 20 km resolution, making use of an oblique Lambert projection with an origin at 56° N, 4° W (center of the BSH North Sea SST analysis). All daily satellite pixels falling into a 20x20 km grid box are considered equally when calculating a weekly average for this particular 20x20 km grid box. Eventually, the result for the weekly average is smoothed using a binomial filter (50 % weight for the grid box itself, 50 % for its respective neighbors). While the processing of the satellite data itself on the 1.1 km grid has been carried out at BSH since 1990, the operational SST analysis for the Baltic Sea did not start until autumn 1996. The analysis of the BSH SST dataset presented in this chapter is therefore constrained to the period 1997–2022.

## 2.2 Station data

In-situ temperature time series from mooring stations which are located in the Baltic Sea are obtained from product ref. no. 2 in Table 1, except for SST data from Northern Baltic (K. Hedi, FMI, pers. communication). Each available dataset has already been quality controlled by the regional production units (In Situ TAC partners, 2022). The temporal resolution varies from hourly data at the German stations and half-hourly at the stations in the northern Baltic Proper and Gulf of Finland. Due to failures, maintenance and other circumstances, no mooring station covers the period from 1st Jan 1993 until now entirely. From all available mooring stations, those are selected which contain data from 2022 and at least ten additional years from 1993 until 2021 in at least one depth. Out of the then remaining seven mooring stations that contained surface temperature data, two mooring stations were chosen for the additional model validation and the analysis of MHWs: Lighthouse Kiel (LT Kiel) and Northern Baltic. LT Kiel has the largest time coverage of observation data (rather continuously from 1989 until the present). It lies in the far western part of the southern Baltic and the water depth at this mooring station is about 12 m. On the other hand, Northern Baltic is located in the northern Baltic Proper and provides measurements down to water depths of 103.8 m. The SST observations there cover the period from 1997 until now, rendering it an ideal candidate for evaluating the effects of MHWs into deeper layers.

## 2.3 Baltic Sea Physics Reanalysis Data

The Baltic Sea physics reanalysis product (product ref. no. 3 in Table 1) is a model dataset produced by using NEMO v4.0, a state-of-the-art oceanographic modeling framework (Gurvan et al., 2019). The model system assimilates satellite observations of SST (EU Copernicus Marine Service Product, 2022b) and in-situ temperature and salinity profile observations from the ICES database (ICES Bottle and low-resolution CTD dataset, 2022). The product provides gridded information on SST and subsurface temperature conditions. The spatial coverage is 1 nm and covers the entire Baltic Sea including the transition zone to the North Sea with a vertical resolution of 56 non-equidistant depth levels. This multi-year product (MYP) covers the reference period from 1993 up to 2022.



## 2.4 Model validation

Although the Baltic Sea physics reanalysis product (product ref. no. 3 in Table 1) has already been extensively validated in  
95 the corresponding Quality Information Document (QuID; Panteleit et al., 2023), the model data is additionally validated for  
this chapter at different mooring stations, in particular LT Kiel and Northern Baltic, using the available station data (product  
ref. no. 2 in Table 1) and the full reference period from 1993 to 2022. Hence, in this case, only mooring stations were  
validated which are mostly located in the southern Baltic, whereas the validation in the QuID also considered ICES data  
which covered the entire Baltic Sea. Our evaluation confirms the results from the QuID, for example, that the MYP  
100 underestimates the temperature at the surface which, on average, results in a negative bias. Nevertheless, as can be clearly  
seen in Fig. 1, the temperature curves at Northern Baltic and LT Kiel, respectively, show the same progression. The  
generally lower temperature in the MYP results in a slightly lower temperature climatology and threshold (here, the 90th  
percentile), respectively, on which the MHW detection is based. In general though, the MHWs and their respective  
intensities and lengths are detected equally in both the station and model data.

105 While the bias at the surface is between  $-0.46\text{ °C}$  and  $-0.2\text{ °C}$ , the bias at deeper levels shifts towards more positive values.  
At the deepest levels where observational data is available, the bias in our validation ranges from  $-0.22\text{ °C}$  to  $0.43\text{ °C}$  which  
also corresponds to the results in the QuID ( $-0.36\text{ °C}$  to  $0.26\text{ °C}$ ). This means that the model bias varies at depth and with  
that maybe also the accuracy. To ensure the quality of the used station data from Northern Baltic, the validation of the lower  
level at the station BMPH2 from the QuID can be used as an approximation. BMPH2 is located only 43 km from Northern  
110 Baltic and reaches a depth of 150 m (in contrast to Northern Baltic with 105 m). It is a monitoring station which is operated  
by vessels and CTD casts are used to obtain measurements. These casts provide measurements at multiple depths, but are  
unevenly distributed over time (Panteleit et al., 2023). Unfortunately, there is no observation data available after 2019. With  
a bias of  $-0.15\text{ °C}$  and a centered pattern root mean square difference (cRMSD) of  $0.17\text{ °C}$  the model data fits quite well to  
the station data (Fig. 1).

## 115 2.5 Heat wave detection

Marine heatwaves (MHWs) refer to a discrete period of unusually high seawater temperatures. While there are several  
definitions to quantitatively describe MHWs, the most commonly used method defines them as periods when temperatures  
exceed the 90th percentile of the local climatology for five days or more (Hobday et al. 2016). Here, we apply the python  
package for MHW detection and statistics by Oliver (2016) to the observational data and the Matlab package by Zhao and  
120 Marin (2019) for the MHW statistics based on the model data. These packages have been shown to produce identical results  
(Zhao and Marin, 2019). The classification of MHWs follows Hobday et al. (2018), where the resulting category is based on  
the maximum intensity in multiples of threshold exceedances, i.e., the local difference between the 90th percentile threshold  
and the climatology. If the threshold is exceeded by less than 2 times this local difference, the MHW is classed as moderate



(Category I), at 2 to 3 times it is classed as strong (Category II), at 3 to 4 times it is classed as severe (Category III) and at 4  
125 times or more as extreme (Category IV).

For the assessment of MHWs in the Baltic domain during 2022 (Sect. 3.2), the climatological data of 1993 to 2022 as well as  
the data of 2022 are collected from the Baltic Sea MYP (product ref. no 3 in Table 1). The following statistical metrics of  
MHW are computed at each available grid point of the reanalysis: cumulative intensity, mean intensity, duration of the  
longest heatwave, number of heatwaves (frequency), maximum intensity and total days of MHW conditions.

130 In order to evaluate the development of MHW metrics over time, block averages (using a block length of one year) for each  
MHW metric are computed for the time series data at the two mooring stations, for both the observations and the model data.  
We then also compute the linear trend (95% significance) for each of those annual MHW metrics. Finally, the correlation of  
the annual MHW metrics to the annual mean temperature based on model data was assessed using a linear least-squares  
regression and a two-sided t-test for significance.

## 135 **3 Results**

### **3.1 Sea surface temperature anomalies**

During summer months, large parts of the Baltic Sea featured strong warm anomalies with highest values of up to 3 °C  
above the long-term mean in the Bothnian Sea in June and the Bothnian Bay in July, respectively (Fig. 2). In August  
however, these areas exhibit rather neutral to cold anomalies, while the Baltic Proper as well as the Gulf of Finland and the  
140 Gulf of Riga show the warmest anomalies of +1.5 °C to 2.5 °C. In the beginning of autumn, the Baltic Sea is marked by a  
substantial east-to-west gradient regarding SST anomalies. This is due to a series of upwelling events along the eastern  
coastlines of the Baltic Sea. In November, again the whole Baltic Sea features strong warm anomalies with peak values  
above +2 °C around Southern Sweden.

To provide some climatological context of the observed SST anomalies, we also present maps of the SST anomaly ranks for  
145 the summer and autumn months in 2022 when compared to their respective months in previous years (right two columns of  
Fig. 2). It is obvious that the warm anomalies found over large parts of the Baltic Sea during summer and autumn 2022  
belong to the warmest eight on record for the respective months. Except for September when the upwelling along the eastern  
coastlines led to cold anomalies contrasting the warm anomalies in the western half of the Baltic Sea, it is found for basically  
all other five months (June through August, as well as October and November) that large areas of the Baltic Sea featured  
150 warm anomalies belonging to the highest four on record. For August and November, we even find several larger areas along  
the coastline of the Baltic countries as well as off the Polish coast and around Gotland that featured surface temperatures  
being the highest ever according to the BSH SST analysis (product ref. no. 1 in Table 1).



### 3.2 Marine heatwaves

Temperature anomalies are a precondition for MHWs. The monthly overview in Fig. 2 already provides an indication of possible MHW conditions. To begin with, these are assessed by using the statistical MHW metrics defined by Hobday et al. (2016) at each grid point based on the SST data extracted from the Baltic Sea MYP (product ref. no. 3 in Table 1). Each region of the Baltic Sea experienced different characteristics during 2022 (Fig. 3).

The most MHWs during 2022 were detected in the Inner Danish Straits and the Western Baltic (Fig. 3d). Mainly 4 to 5 MHWs were detected. At some assessed grid points, up to 7 MHWs are detected, which leads to a maximum of 96 total days of MHW conditions in that area (Fig. 3f). The mean and maximum intensity of all heatwaves in these areas reached up to 3.8 °C and 4.6 °C, respectively (Fig. 3b and 3e). The highest values in mean and maximum intensity of MHWs were reached in the Northern Baltic Proper (up to 5.3 °C, resp. 7.3 °C) as well as the Gulf of Bothnia (up to 6.5 °C, resp. 9.6 °C). The maximum intensities were even the highest within the entire studied period from 1993 to 2022. Those regions were impacted by mainly two MHWs, but at some individual grid points up to six MHWs are identified with a maximum value of up to 63 days with MHW qualification. While the duration of the longest MHW is similar in both regions (Fig. 3c), the highest values of cumulative intensity (of a single MHW) are found in the Gulf of Bothnia in the Kvarken (up to 119.3 days °C), while the values in the Western Baltic and Inner Danish Straits are lower (up to 64 days °C) (Fig. 3a).

Compared with Fig. 2, the MHW with the highest cumulative intensity in the Gulf of Bothnia derives from the temperature anomaly in November. The numerous MHWs in the Western Baltic and the large number of days with MHW conditions connected with them occurred in both the summer and autumn months.

#### 3.2.1 Multi-year evaluation of MHW metrics

Next, we assess the frequency and other characteristics of MHWs that occurred in 2022 in a climatological context based on both observations and model data for the two stations LT Kiel (for the overlapping period 1993–2022, Fig. 4a–h) and Northern Baltic (for the overlapping period 1997–2022, Fig. 4 i–p).

In 2022, in total five MHWs occurred at LT Kiel, spread out through the year (Fig. 1a). Though none of the 2022 MHWs was extraordinarily long or intense, the station data shows that the number of MHW occurrences was the second highest after 2020 (Fig. 4a). The time series of MHW frequency per year suggests that the occurrence of MHW events has increased over the last three decades (Fig. 4a). This trend of +0.7 MHWs per decade becomes statistically significant when all the available station data from 1989–2022 is taken into account. The number of MHW events per year is positively correlated ( $R=0.76$ ) with the increasing annual mean SST at that mooring station (Fig. 4b). The maximum (Fig. 4c) and cumulative intensities (Fig. 4e) of observed MHWs do not show a clear trend and are not correlated to rising mean temperatures (Fig. 4d and Fig. 4f). There is no significant trend in total MHW days (Fig. 4g) at LT Kiel but a positive correlation ( $R=0.71$ ) with rising average temperatures (Fig. 4h).



For Northern Baltic, neither the station data nor the model data exhibits a statistically significant trend in MHW events for  
185 the overlapping period (Fig. 4i). But when all of the available model data from 1993–2022 is taken into account, the trend in  
MHW occurrences becomes significant at the 95 % level with +0.64 MHWs per decade. Again, the number of events is  
positively correlated with annual mean temperature ( $R=0.58$ , Fig. 4j). The highest maximum MHW intensities were recorded  
in recent years (2016, 2018, 2021, 2022) with 2022 showing the highest intensity of a MHW with 7.3 °C (model data) to  
7.4 °C (station data) above the climatologically expected temperature (Fig. 4k,l, see also Fig. 1b). The cumulative MHW  
190 intensities show no clear trend or correlation with annual mean temperatures at this station (Fig. 4m,n). In terms of total  
MHW days, 2018 was exceptional (Fig. 4o), but otherwise no trend is detectable for this metric, though there is positive  
correlation with annual mean temperatures ( $R=0.56$ , Fig. 4p).

### 3.2.2 Analysis of vertical MHW distribution at Northern Baltic

At Northern Baltic, which is more than 104 m deep and located in the Western Baltic Proper, the surface temperature has  
195 been continuously measured over several decades. Unfortunately, no temperature measurements exist in lower layers. In  
Sect. 2.4 we showed that the model data coincides well with observational data, both at the surface and in the lower layers.  
Thus, in order to obtain further insights into the heat wave propagation towards the seafloor, we analyzed the MYP model  
data (product ref. no. 3 in Table 1) along the entire water column.

A seasonal SST signal is clearly visible in Fig. 5a. In general, the temperature tends to decrease with depth while the bottom  
200 temperature is relatively cold and uniform. In late spring (June), a so-called cold intermediate layer (CIL) at a depth of  
20–60 m, which is defined as a minimum of temperature between the thermocline and the perennial halocline (Chubarenko et  
al., 2017; Dutheil et al., 2022), is formed. The upper boundary of the CIL is in good agreement with the mixed layer depth.  
The CIL acts as a barrier between the surface and bottom water body and has a significantly lower temperature (Fig. 5b)  
of -0.3 °C to 4.5 °C as the climatological mean. As shown in Fig. 5c and Fig. 5d, the intensity of the MHW tends to decrease  
205 as the depth increases. MHWs in regions close to the seafloor were detected during specific periods from February to April,  
September to October and in December. During July, a one day extreme MHW (Category IV) event was observed at the  
surface with 7.4 °C above the climatological mean temperature, followed by further three days with a severe MHW  
(Category III). A few weeks prior to this MHW (and in 10.8 m depth also afterwards), the temperature was already  
significantly higher than the climatological mean, but not high enough to result in a MHW (Fig. 5e and 5f). The elevated  
210 temperatures started with a significant temperature jump of 5 °C above the climatological mean, followed by an abrupt and  
substantial increase and decrease in temperature over a short period (Fig. 5e). Following this extreme heatwave event, a  
comparably weaker MHW is observed in mid-August. The weaker August MHW is observable at 0.5 m (Fig. 5e) and 10.8 m  
(Fig. 5f), while the June MHW is already no longer noticeable below the mixed layer depth.





#### 4 Discussion and Conclusions

215 During August and November 2022 record warm sea surface temperatures were observed in substantial areas in the Baltic  
Sea proper. Large parts of the Baltic Sea exhibited the third-warmest to the warmest summer or autumn temperatures since  
1997. Both periods in August and November coincided with atmospheric temperature anomalies. In August air temperatures  
were higher than the 1991–2020 average across most of Europe, especially in Eastern Europe, in a band stretching from the  
Barents and Kara seas to the Caucasus (Copernicus Climate Change Service/ECMWF, 2022a). In November 2022, air  
220 temperatures were higher than the 1991–2020 average especially over the west, south-east and far north of Europe and  
unusually mild over the northern European seas (Copernicus Climate Change Service/ECMWF, 2022b). These atmospheric  
surface temperature anomalies are a likely driver for MHWs since they seem to coincide with the observed marine surface  
temperature anomalies. Holbrook et al. (2019) found that the MHWs they studied at middle and high latitude regions were  
driven by large-scale atmospheric pressure anomalies which cause anomalous ocean warming. Stalled ridges of atmospheric  
225 high-pressure systems coincide with clear skies, warm air, and reduced wind speeds. These conditions lead to quick warming  
of the upper ocean and increase thermal stratification due to reduced vertical mixing.

In 2022, MHWs occurred in all marginal seas of Europe where the Baltic Sea was not an exception. The distribution of  
quantity and intensity of MHWs within the Baltic Sea is twofold: Up to seven individual MHW occurrences were both  
recorded and simulated in the south-western part of the Baltic Sea, which lead to the fact that this region experienced the  
230 maximum number of total MHW days in the Baltic Sea in 2022. In the northern part, the total number of MHWs was lower,  
with locally only one MHW being detected. Remarkably, this MHW also led to the highest mean and maximum MHW  
intensities in the Baltic Sea since the reanalysis started in 1993: In some areas, temperatures exceeded 9 °C above the 90th  
percentile of the climatologically expected temperature values.

At our two exemplary stations a significant increase of MHW occurrences is detectable over time: +0.7 MHW events per  
235 decade at LT Kiel and +0.64 MHW events per decade at Northern Baltic. There is a statistical relationship between both  
MHW frequency and total number of MHW days with rising mean temperatures. This confirms that, also in the Baltic Sea,  
an increasing number of MHWs can be expected in the future due to global warming (Frölicher et al., 2018; Oliver et al.,  
2019). Adverse impact of MHWs to different trophic levels of the ecosystem is widely documented (Smale et al., 2019;  
IPCC, 2022; Smith et al., 2023). The Baltic Sea, which has a relatively vulnerable ecosystem, could experience significant  
240 negative impact due to MHWs (Kauppi and Villnäs, 2022; Kauppi et al., 2023).

Potential for future studies opens up by examining whether the August MHW in 2022 could propagate to the deeper water  
masses close to the halocline at Northern Baltic and also regarding the correlation between the propagation into deeper water  
masses and the strength (i.e. classification) of the MHW. Further studies could determine if the positive feedback on the  
bottom temperature, that was observed in 2022, can also be found in following years and whether this phenomenon is  
245 triggered by the superposition of lateral currents and/or MHWs. Understanding the effects that potentially led to the vertical





propagation of MHWs, particularly in late summer, will become increasingly crucial in order to evaluate the effects of the already rising occurrence of surface MHWs with respect to their impact on the ecosystem in subsurface layers.

### **Data availability**

This study is based on public databases and the references are listed in Table 1.

### 250 **Author contribution**

The idea and concept of this chapter was formed by Anja Lindenthal, Claudia Hinrichs, Priidik Lagemaa, Helen E. Morrison and Urmas Raudsepp. The data curation was done by Eefke M. van der Lee and Tim Kruschke for the data from product ref. no. 1 in Table 1, by Claudia Hinrichs and Tabea R. Panteleit for the data from product ref. no. 2 in Table 1 and by Simon Jandt-Scheelke and Tabea R. Panteleit for the data from product ref. no. 3 in Table 1. The formal analyses of the datasets and  
255 the resulting investigations were performed by Anja Lindenthal, Claudia Hinrichs, Simon Jandt-Scheelke, Tim Kruschke and Tabea R. Panteleit. Additional model validation was performed by Tabea R. Panteleit. Claudia Hinrichs, Simon Jandt-Scheelke, Tim Kruschke and Tabea R. Panteleit were responsible for the visualization of the data. Anja Lindenthal, Claudia Hinrichs, Simon Jandt-Scheelke, Tim Kruschke, Eefke M. van der Lee, Tabea R. Panteleit and Urmas Raudsepp were involved in the original draft preparation, while the manuscript was finally reviewed and edited by Claudia Hinrichs, Priidik  
260 Lagemaa, Helen E. Morrison and Urmas Raudsepp with contributions from all co-authors.

### **Competing interests**

The authors declare that they have no conflict of interest.

### **Funding**

This work is supported by the Copernicus Marine Service for the Baltic Sea Monitoring and Forecasting Center (21002L2-  
265 COP-MFC BAL-5200).

### **References**

Belkin, I. M.: Rapid warming of large marine ecosystems. *Progress in Oceanography*, 81(1-4), 207-213, <https://doi.org/10.1016/j.pocean.2009.04.011>, 2009.



- Cheng, L., von Schuckmann, K., Abraham, J. P., et al.: Past and future ocean warming, *Nature Reviews Earth and Environment*, 3(11), 776-794, <https://doi.org/10.1038/s43017-022-00345-1>, 2022.
- 270
- Chubarenko, I. P., Demchenko, N. Y., Esiukova, E. E., Lobchuk, O. I., Karmanov, K. V., Pilipchuk, V. A., Isachenko, I. A., Kuleshov, A. F., Chugaevich, V. Y., Stepanova, N. B. et al.: Spring thermocline formation in the coastal zone of the southeastern Baltic Sea based on field data in 2010–2013. *Oceanology*, 57, 632–638, <https://doi.org/10.1134/S000143701705006X>, 2017.
- 275 Copernicus Climate Change Service/ECMWF, <https://climate.copernicus.eu/surface-air-temperature-august-2022>, last access: 11 July 2023, 2022a.
- Copernicus Climate Change Service/ECMWF, <https://climate.copernicus.eu/surface-air-temperature-november-2022>, last access: 11 July 2023, 2022b.
- Dutheil, C., Meier, H. E. M., Gröger, M., Börgel, F.: Warming of Baltic Sea water masses since 1850, *Climate Dynamics*, 280 <https://doi.org/10.1007/s00382-022-06628-z>, 2022.
- EU Copernicus Marine Service Product: Global Ocean- In-Situ Near-Real-Time Observations, Mercator Ocean International, [data set], <https://doi.org/10.48670/moi-00036>, 2022a.
- EU Copernicus Marine Service Product: Baltic Sea - L3S Sea Surface Temperature Reprocessed, Mercator Ocean International, [data set], <https://doi.org/10.48670/moi-00312>, 2022b.
- 285 EU Copernicus Marine Service Product: Baltic Sea Physics Reanalysis, Mercator Ocean International, [data set], <https://doi.org/10.48670/moi-00013>, 2023.
- EUMETSAT, AVHRR Factsheet, Doc.No.: EUM/OPS/DOC/09/5183, <https://www.eumetsat.int/media/39253>, 2015.
- Frölicher, T. L., Fischer, E. M., Gruber, N.: Marine heatwaves under global warming, *Nature*, 560, 360–364, <https://doi.org/10.1038/s41586-018-0383-9>, 2018.
- 290 Goebeler, N., Norkko, A., Norkko, J.: Ninety years of coastal monitoring reveals baseline and extreme ocean temperatures are increasing off the Finnish coast, *Commun. Earth Environ.*, 3, 215, <https://doi.org/10.1038/s43247-022-00545-z>, 2022.
- Gröger, M., Placke, M., Meier, H. E. M., Börgel, F., Brunnabend, S.-E., Dutheil, C., Gräwe, U., Hieronymus, M., Neumann, T., Radtke, H., Schimanke, S., Su, J., Väli, G.: The Baltic Sea Model Intercomparison Project (BMIP) – a platform for model



- development, evaluation, and uncertainty assessment, *Geosci. Model Dev.*, 15, 8613–8638, <https://doi.org/10.5194/gmd-15-8613-2022>, 2022.
- 295
- Gurvan, M., Bourdallé-Badie, R., Chanut, J., Clementi, E., Coward, A., Ethé, C., Iovino, D., Lea, D., Lévy, C., Lovato, T., Martin, N., Masson, S., Mocavero, S., Rousset, C., Storkey, D., Vancoppenolle, M., Müeller, S., Nurser, G., Bell, M., Samson, G.: NEMO ocean engine. In Notes du Pôle de modélisation de l'Institut Pierre-Simon Laplace (IPSL) (v4.0, Number 27). Zenodo. <https://doi.org/10.5281/zenodo.3878122>, 2019.
- 300 Hobday, A. J., Alexander, L. V., Perkins, S. E., Smale, D. A., Straub, S. C., et al.: A hierarchical approach to defining marine heatwaves, *Prog. Oceanogr.*, 141, 227–38, <https://doi.org/10.1016/j.pocean.2015.12.014>, 2016.
- Hobday, A. J., Oliver, E. C. J., Sen Gupta, A., Benthuisen, J. A., Burrows, M. T., Donat, M. G., Holbrook, N. J., Moore, P. J., Thomsen, M. S., Wernberg, T., Smale, D. A.: Categorizing and naming marine heatwaves, *Oceanography*, 31(2), 162–173, <https://doi.org/10.5670/oceanog.2018.205>, 2018.
- 305 Holbrook, N.J., Scannell, H.A., Sen Gupta, A., Benthuisen, J.A., Feng, M., Oliver, E.C., Alexander, L.V., Burrows, M.T., Donat, M.G., Hobday, A.J. and Moore, P.J.. A global assessment of marine heatwaves and their drivers. *Nature communications*, 10(1), p.2624. <https://doi.org/10.1038/s41467-019-10206-z>. 2019.
- ICES Bottle and low-resolution CTD dataset, Extractions 22 DEC 2013 (for years 1990-20012), 25 FEB 2015 (for year 2013), 13 OCT 2016 (for year 2015), 15 JAN 2019 (for years 2016-2017), 22 SEP 2020 (for year 2018), 10 MAR 2021 (for years 2019-202), 28 FEB 2022 (for year 2021), ICES, Copenhagen, 2022.
- 310
- In Situ TAC partners: EU Copernicus Marine Service Product User Manual for the Global Ocean- In-Situ Near-Real-Time Observations Product, INSITU\_GLO\_PHYBGCWAV\_DISCRETE\_MYNRT\_013\_030, Issue 1.14, Mercator Ocean International, <https://catalogue.marine.copernicus.eu/documents/PUM/CMEMS-INS-PUM-013-030-036.pdf>, last access: 12 April 2023, 2022.
- 315 IPCC: Climate Change 2022: Impacts, Adaptation, and Vulnerability. Contribution of Working Group II to the Sixth Assessment Report of the Intergovernmental Panel on Climate Change, eds.: Pörtner, H.-O., Roberts, D. C., Tignor, M., Poloczanska, E. S., Mintenbeck, K., Alegría, A., Craig, M., Langsdorf, S., Löschke, S., Möller, V., Okem, A., Rama, B., Cambridge University Press, Cambridge, UK and New York, NY, USA, 3056 pp., <https://doi.org/10.1017/9781009325844>, 2022.



- 320 Kauppi, L., Villnäs, A.: Marine heatwaves of differing intensities lead to distinct patterns in seafloor functioning, *Proceedings of the Royal Society B: Biological Sciences*, 289(1986), 20221159, <https://doi.org/10.1098/rspb.2022.1159>, 2022.
- Kauppi, L., Göbeler, N., Norkko, J., Norkko, A., Romero-Ramirez, A., Bernard, G.: Changes in macrofauna bioturbation during repeated heatwaves mediate changes in biogeochemical cycling of nutrients, *Frontiers in Marine Science*, 9, 1070377, 325 <https://doi.org/10.3389/fmars.2022.1070377>, 2023.
- Minnett, P. J., Alvera-Azcárate, A., Chin, T. M., Corlett, G. K., Gentemann, C. L., Karagali, I., Li, X., Marsouin, A., Marullo, S., Maturi, E., Santoleri, R., Saux Picart, S., Steele, M., Vazquez-Cuervo, J.: Half a century of satellite remote sensing of sea-surface temperature, *Remote Sensing of Environment*, 233, 111366, ISSN 0034-4257, <https://doi.org/10.1016/j.rse.2019.111366>, 2019.
- 330 Oliver, E. C. J.: marineHeatWaves v0.16, github [code], <https://github.com/ecjoliver/marineHeatWaves>, 2016.
- Oliver, E. C. J.: Mean warming not variability drives marine heatwave trends, *Clim. Dyn.*, 53, 1653–1659, <https://doi.org/10.1007/s00382-019-04707-2>, 2019.
- Panteleit, T., Verjovkina, S., Jandt-Scheelke, S., Spruch, L. and Huess, V.: EU Copernicus Marine Service Quality Information Document for the Baltic Sea Physics Reanalysis Product, BALTICSEA\_MULTIYEAR\_PHY\_003\_011, Issue 335 4.0, Mercator Ocean International, <https://catalogue.marine.copernicus.eu/documents/QUID/CMEMS-BAL-QUID-003-011.pdf>, last access: 12 April 2023, 2023.
- Raudsepp, U., Maljutenko, I., Haapala, J., Männik, A., Verjovkina, S., Uiboupin, R., von Schuckmann, K., Mayer, M.: Record high heat content and low ice extent in the Baltic Sea during winter 2019/20. In: Copernicus Ocean State Report, Issue 6, *Journal of Operational Oceanography*, 15:sup1, s175–s185, <https://doi.org/10.1080/1755876X.2022.2095169>, 2022.
- 340 Ringgaard, I., Korabel, V., Spruch, L., Lindenthal, A. and Huess, V.: EU Copernicus Marine Service Product User Manual for the Baltic Sea Physics Reanalysis Product, BALTICSEA\_MULTIYEAR\_PHY\_003\_011, Issue 1.0, Mercator Ocean International, [https://catalogue.marine.copernicus.eu/documents/PUM/CMEMS-BAL-PUM-003-011\\_012.pdf](https://catalogue.marine.copernicus.eu/documents/PUM/CMEMS-BAL-PUM-003-011_012.pdf), last access: 12 April 2023, 2023.
- She, J., Su, J., Zinck, A.-S.: Anomalous surface warming in the Baltic Sea in summer 2018 and mechanism analysis, In: 345 Copernicus Marine Service Ocean State Report, Issue 4, *Journal of Operational Oceanography*, 13:sup1, s125–s132; <https://doi.org/10.1080/1755876X.2020.1785097>, 2020.



- Smale, D. A., Wernberg, T., Oliver, E. C. J., et al.: Marine heatwaves threaten global biodiversity and the provision of ecosystem services, *Nature Climate Change*, 9(4), 306-312, <https://doi.org/10.1038/s41558-019-0412-1>, 2019.
- Smith, K. E., Burrows, M. T., Hobday, A. J., King, N. G., Moore, P. J., Gupta, A. S., Thomsen, M. S., Wernberg, T., Smale, D. A.: Biological Impacts of Marine Heatwaves. *Annual Review of Marine Science*, 15 (1), 119–145. <https://doi.org/10.1146/annurev-marine-032122-121437>, 2023.
- Sun, D., Jing, Z., Li, F., Wu, L.: Characterizing global marine heatwaves under a spatio-temporal framework, *Progress in Oceanography*, 211, 102947, <https://doi.org/10.1016/j.pocean.2022.10294>, 2023.
- The BACC Author Team: Assessment of Climate Change for the Baltic Sea Basin, Springer Berlin, Heidelberg, p. 88, <https://doi.org/10.1007/978-3-540-72786-6>, 2008.
- Väli, G., Meier, H. M., Elken, J.: Simulated halocline variability in the Baltic Sea and its impact on hypoxia during 1961–2007, *J. Geophys. Res. Oceans*, 118, 6982-7000, <https://doi.org/10.1002/2013JC009192>, 2013.
- Wehde, H., Schuckmann, K. V., Pouliquen, S., Grouazel, A., Bartolome, T., Tintore, J., De Alfonso Alonso-Munoyerro, M., Carval, T., Racapé, V. and the INSTAC team: EU Copernicus Marine Service Quality Information Document for the Global Ocean- In-Situ Near-Real-Time Observations Product, INSITU\_GLO\_PHYBGCWAV\_DISCRETE\_MYNRT\_013\_030, Issue 2.2, Mercator Ocean International, <https://catalogue.marine.copernicus.eu/documents/QUID/CMEMS-INS-QUID-013-030-036.pdf>, last access: 12 April 2023, 2022.
- WMO: State of the Global Climate 2022, WMO-No. 1316, World Meteorological Organization, 2023, 48 pp., 2023.
- Zhao, Z., Marin, M.: A MATLAB toolbox to detect and analyze marine heatwaves, *Journal of Open Source Software*, 4(33), 1124, <https://doi.org/10.21105/joss.01124>, 2019.



**Table 1: Product Table**

Product ref. no.	Product ID & type	Data access	Documentation
1	BSH Sea Surface Temperature (AVHRR/3); Satellite data	Upon request; overview and contact data via <a href="https://www.bsh.de/EN/TOPICS/Monitoring_systems/Remote_sensing/remote_sensing_node.html">https://www.bsh.de/EN/TOPICS/Monitoring_systems/Remote_sensing/remote_sensing_node.html</a>	<a href="https://www.bsh.de/DE/THEMEN/Beobachtungssysteme/Fernerkundung/fernerkundung_node.html">https://www.bsh.de/DE/THEMEN/Beobachtungssysteme/Fernerkundung/fernerkundung_node.html</a>
2	INSITU_GLO_PHYBGCWAV_DISCRETE_MYNRT_013_030; In-Situ Near-Real-Time Observations	<a href="#">EU Copernicus Marine Service Product (2022a)</a>	Quality Information Document (QUID): <a href="#">Wehde et al., 2022</a>  Product User Manual (PUM): <a href="#">In Situ TAC partners, 2022</a>
3	BALTICSEA_MULTIYEAR_PHY_003_011; Numerical models	<a href="#">EU Copernicus Marine Service Product (2023)</a>	Quality Information Document (QUID): <a href="#">Panteleit et al., 2023</a>  Product User Manual (PUM): <a href="#">Ringgaard et al., 2023</a>

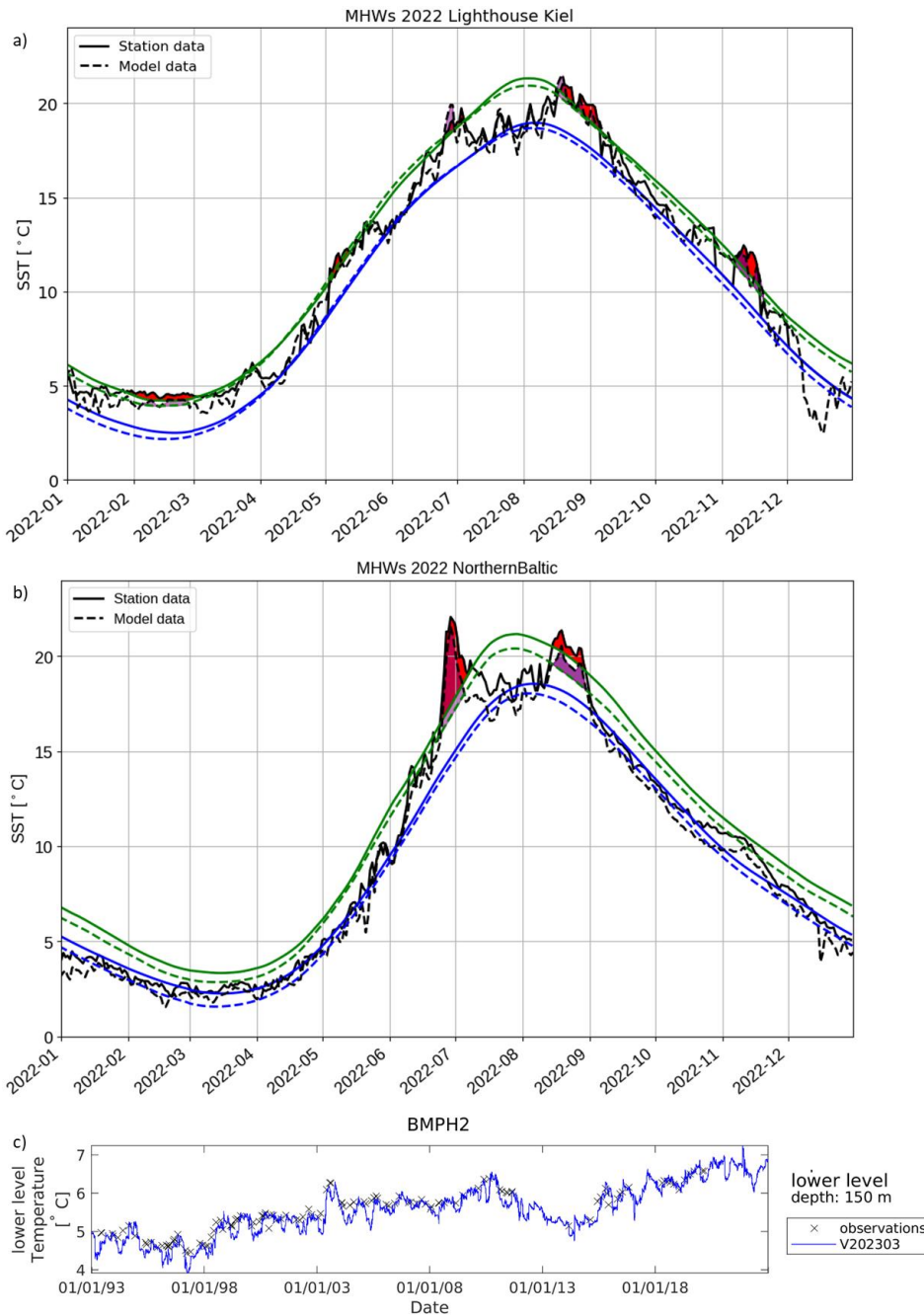
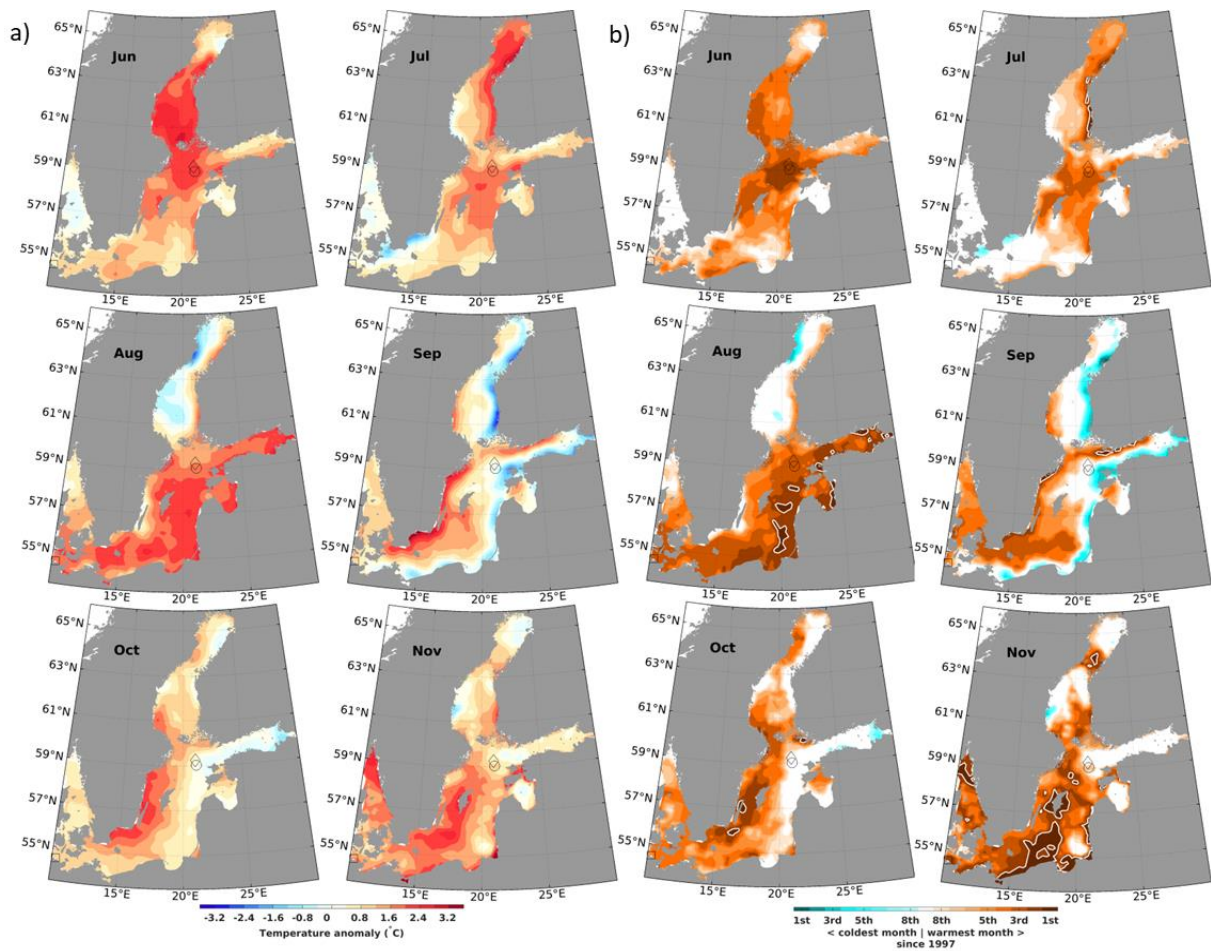


**Figure 1:** Comparison of station data with model data at (a) LT Kiel (product ref. no. 2 and 3 in Table 1), (b) Northern Baltic (product ref. no. 2 and 3 in Table 1) and (c) BMPH2 (from Panteleit et al., 2023). The dashed lines in (a) and (b) correspond to the model (product ref. no. 3 in Table 1), while the continuous lines correspond to the station data (product ref. no. 2 in Table 1). In blue, the climatological mean is shown. The green lines show the 90th percentile threshold for MHW detection and the black lines are the respective 2022 temperature data. The purple (model data) and red (station data) marked areas show the detected MHWs in 2022. The reference period for LT Kiel (a) is 1993-2021 and 1997-2021 for Northern Baltic (b). (c) shows the validation at the station BMPH2 at a depth of 150 m. The model data is shown in blue and the measured data are displayed with the black crosses.

375

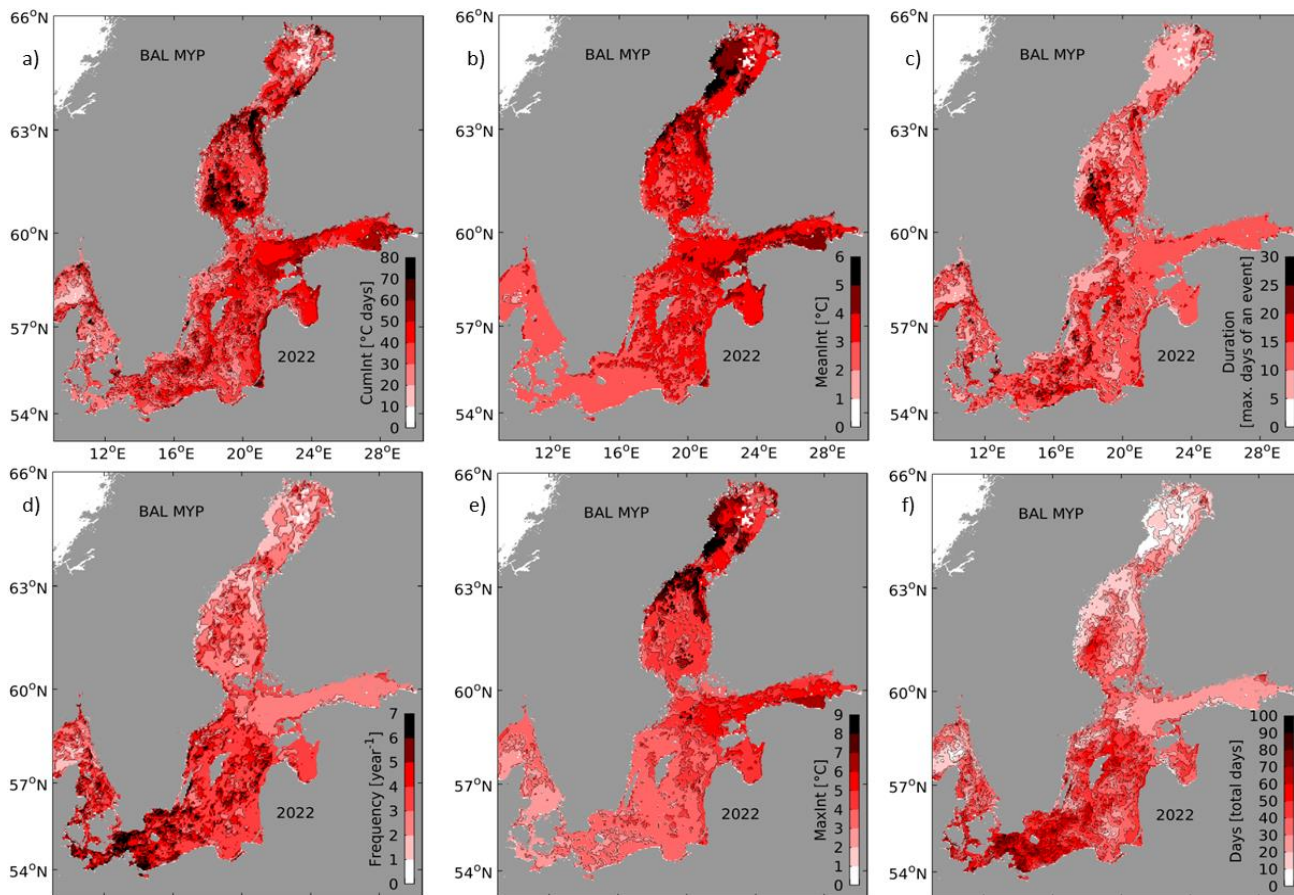




380

**Figure 2: Anomalies (difference to climatology of 1997-2021) of SST for the Baltic Sea according to the BSH SST analysis (product ref. no 1 in Table 1) during the summer and autumn months in 2022 (a) and ranks of these SST anomalies (b) when compared to the full dataset starting in 1997. In (b), Brownish (cyan) colors denote anomalies belonging to the warmest (coldest) eight anomalies found since 1997. Record warm anomalies (rank 1) are highlighted by white contours. Locations of the in-situ observations discussed in this chapter are marked by a square (LT Kiel), a diamond (Northern Baltic), and a circle (BMPH2), respectively.**

385



390 **Figure 3: Statistical metrics of MHWs in 2022 in the Baltic Sea based on SST data of the Baltic Sea MYP (product ref. no. 3 in Table 1) covering the years 1993 to 2022 - (a) cumulative intensity of the longest heatwave, (b) mean intensity, (c) duration of the longest heatwave, (d) number of heatwaves during 2022, (e) maximum intensity during the longest heatwave, (f) summed up days of all heatwave during 2022. The definition of these metrics follows [Hobday et al. \(2016\)](#).**



### LT Kiel

### Northern Baltic

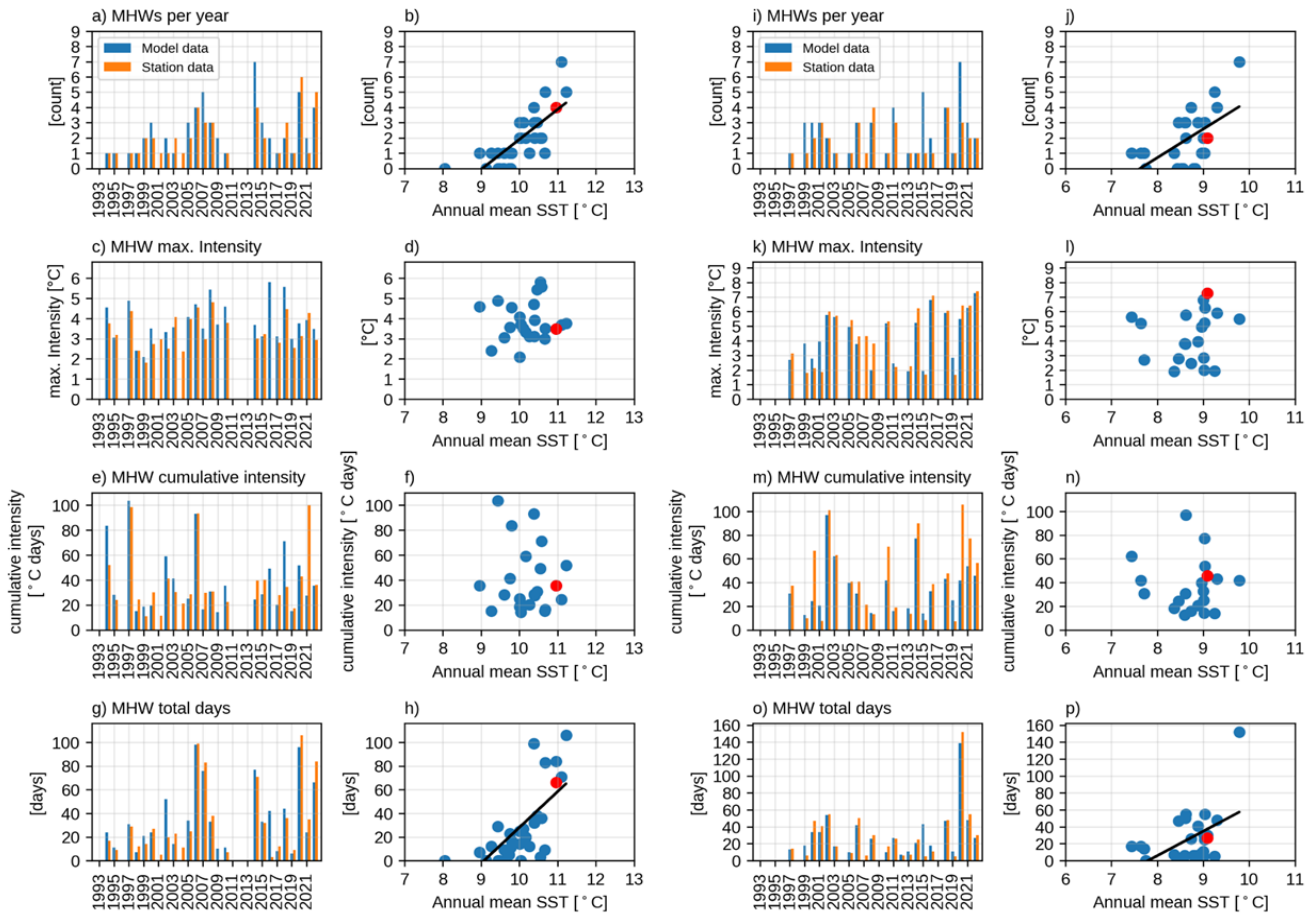


**Figure 4: Comparison and time series of annual MHW metrics (a,i: MHW events; c,k: maximum intensity [°C]; e,m: cumulative intensity [°C days]; g,o: MHW days) for station data (orange bars) and model data (blue bars) at the stations LT Kiel (left) and Northern Baltic (right). The MHW metrics from the model are plotted against the annual mean SST at that station with the year 2022 marked in red. Statistically significant (95 %) correlations are indicated with a black line.**

395

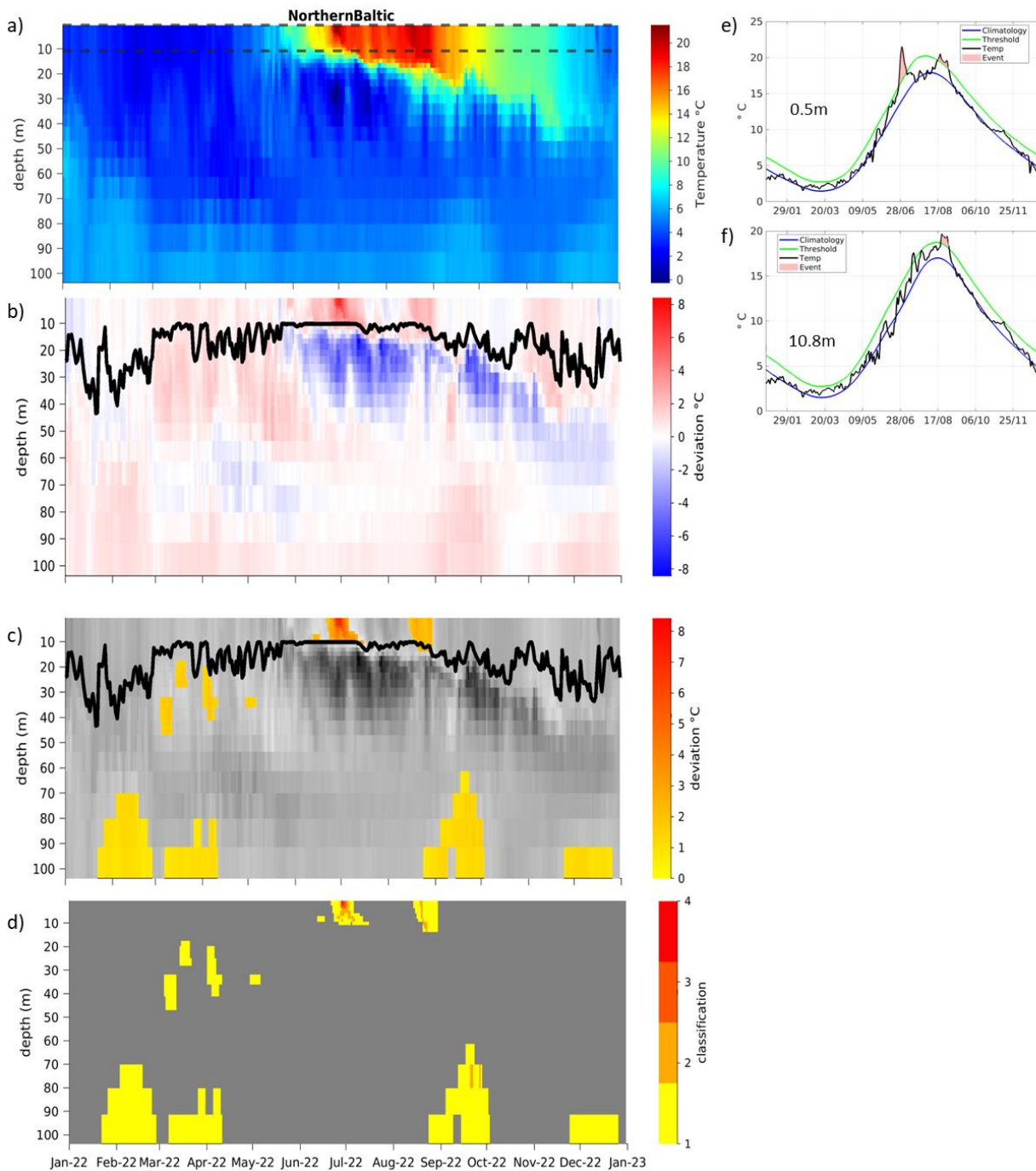


**Figure 5:** Hovmöller diagrams show water temperature (a), temperature anomalies (b) and MHWs (c) and their classifications (d, 1-moderate, 2-strong, 3-severe, 4-extreme) including the mixed layer depth (b and c) at Northern Baltic based on the Baltic Sea MYP (product ref. no. 3 in Table 1). The time series on the right (e-h) are located at the vertical positions marked as dashed lines in (a) and show SST (black), climatology (blue), 90<sup>th</sup> percentile threshold for MHW analysis (green) and MHWs (red shading) based on model data at depths of 0.5 m (e), 10.8 m (f), 80.1 m (g) and 103.8 m (h). The period used for the climatology is 1993-2021.

400